ADP Inhibition of Myosin V ATPase Activity

Enrique M. De La Cruz, H. Lee Sweeney, and E. Michael Ostap

University of Pennsylvania School of Medicine, Department of Physiology, and the Pennsylvania Muscle Institute, Philadelphia, Pennsylvania 19104-6085 USA

ABSTRACT   The kinetic mechanism of myosin V is of great interest because recent evidence indicates that the two-headed myosin V molecule functions as a processive motor, i.e., myosin V is capable of moving along an actin filament for many catalytic cycles of the motor without dissociating. Three recent publications assessing the kinetics of single-headed myosin V provide different conclusions regarding the mechanism, particularly the rate-limiting step of the cycle. One study (De La Cruz et al., 1999, *Proc. Natl. Acad. Sci. USA.* 96:13726–13731) identifies ADP release as the rate-limiting step and provides a kinetic explanation for myosin V processivity. The others (Trybus et al., 1999, *J. Biol. Chem.* 274:27448–27456; Wang et al., 2000, *J. Biol. Chem.* 275:4329–4335) do not identify the rate-limiting step but conclude that it is not ADP release. We show experimental and simulated data demonstrating that the inconsistencies in the reports may be due to difficulties in the measurement of the steady-state ATPase rate. Under standard assay conditions, ADP competes with ATP, resulting in product inhibition of the ATPase rate. This presents technical problems in analyzing and interpreting the kinetics of myosin V and likely of other members of the myosin family with high ADP affinities.

INTRODUCTION

The myosin superfamily of actin-based motor proteins is currently known to include at least 15 classes. The cellular roles of these myosins are likely to be extremely varied (Mooseker and Cheney, 1995), which undoubtedly requires both structural and enzymatic specializations. In the specific case of myosin V, a recent report demonstrates that a single, two-headed molecule is capable of moving an actin filament and able to move along an actin filament for several ATP-driven cycles before dissociating (Mehta et al., 1999). This confirms much speculation that myosin V is a processive motor, based on its role in vesicle trafficking (Titus, 1997).

consistent with the observed processivity of the native two-headed molecule (De La Cruz et al., 1999). The myosin V construct characterized consists of the motor with one of six light-chain/calmodulin-binding domains, or IQ motifs and a tightly bound essential light chain. We refer to this as myosin V-1IQ. While the overall ATPase mechanism (Scheme 1) is conserved among all characterized myosins, the rate constants of the myosin-V ATPase are significantly different from those characterized previously. The key features of the myosin-V kinetic mechanism are (De La Cruz et al., 1999): 1) rate-limiting ADP release (k_{+5}') when bound to
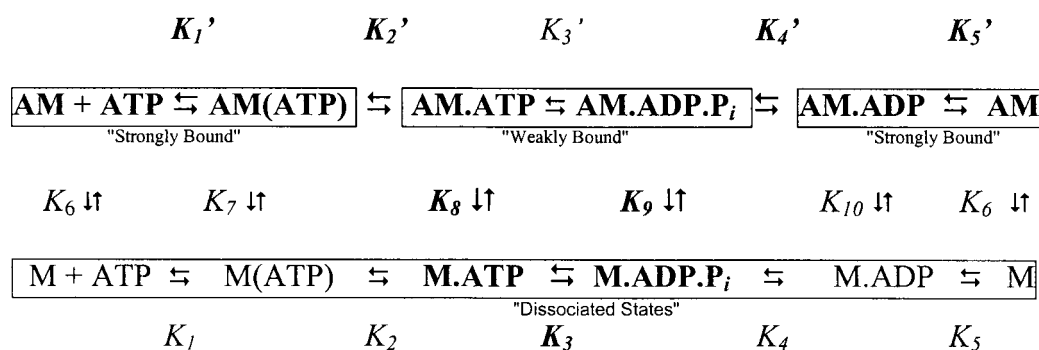
We determined the rate constants for a single-headed myosin V motor ATPase cycle and provided a mechanism

Scheme 1

actin; 2) a high ADP affinity, both on (K_5') and off (K_5) actin; 3) a rapid ATP hydrolysis ($k_{+3} + k_{-3}$); and 4) a rapid (non-rate-limiting) P_i release (k_{+4}') on actin. The key differences in myosin V compared with other myosins is that ADP dissociation in the presence of actin is slow and rate-limiting, and ATP hydrolysis and P_i release are at least 10-fold faster than ADP release.

The rate of phosphate release limits the rate of transition from states that are weakly attached to actin (and thus do not support load) to states that are strongly attached to actin

(Scheme 1). The rate of ADP release limits the rate of transition from the strongly bound states to the weakly bound states. For skeletal muscle myosin II, P_i release limits the steady-state ATPase cycle, and thus the predominant steady-state intermediates are either detached or weakly attached to actin (Scheme 1). Thus the implication of changing the rate-limiting step to ADP release (k'_{+5}) is that it creates a myosin that spends the vast majority of its actin-activated cycle in state(s) that are strongly bound to actin (i.e., a motor with a high duty ratio).

Two other reports on the kinetics of single-headed myosin V (Trybus et al., 1999; Wang et al., 2000) do not support our conclusions or the conclusion that myosin V is a processive motor. While neither study included direct measurements of ATP hydrolysis or the rate of P_i release, both reported ADP release rates that were considerably faster than the steady state ATPase rate and concluded that ADP release was not rate-limiting in the actomyosin V ATPase cycle. While this may reflect isoform differences, this seems unlikely, given that most of the kinetic parameters measured are in general agreement (Table 1), with the major exception of the steady-state ATP hydrolysis rate (Table 1). In this report, we provide data and kinetic simulations demonstrating that the steady-state rates measured by Trybus et al. (1999) and Wang et al. (2000) may be artifactually low and

are likely to be consistent with ADP release being the rate-limiting step in the myosin V kinetic cycle generating a motor with a high duty ratio (De La Cruz et al., 1999).

EXPERIMENTAL PROCEDURES

Proteins and reagents

All reagents were of the highest purity available. ATP was purified by anion exchange chromatography (>99.5% purity), and the concentration was determined by absorbance at 259 nm, using $\epsilon_{259} = 15.4$ mM^{-1} cm^{-1}. In some cases, ATP (>99.7% purity confirmed by high-performance liquid chromatography (HPLC); Roche Biochemicals) was used without further purification, with identical results. Actin was purified from rabbit skeletal muscle and gel filtered (MacLean-Fletcher and Pollard, 1980). Ca-actin was converted to Mg-Actin with 0.2 mM EGTA and 50 μM MgCl$_2$ before polymerization by dialysis against three changes of 0.5 L of KMg50 buffer (50 mM KCl, 1 mM MgCl$_2$, 1 mM EGTA, 1 mM DTT, 10 mM imidazole (99+%), pH 7.0). Phalloidin was used to stabilize actin filaments. A construct consisting of the myosin V motor domain and the first IQ motif (myosin V-1IQ) with bound essential light chain (LC-1sa) was expressed and purified as described (De La Cruz et al., 1999).

Quench flow kinetics and simulations

ATP hydrolysis measurements were made at 25°C in KMg50 buffer with a KINTEK (Austin, Texas) RQF-3 quench flow apparatus, using [γ-^{32}P]ATP (De La Cruz et al., 1999). Actomyosin V-1IQ solutions were treated with 0.002 U ml^{-1} apyrase (potato grade VII, high ADP:ATP ratio) for 30 min on ice before use. ATP hydrolysis by phalloidin-stabilized actin filaments treated with apyrase was minimal during the time course of the experiment and was subtracted from the data in the presence of myosin. Kinetic modeling and simulations (De La Cruz et al., 1999) were performed using a complete (Scheme 1) or simplified (Scheme 2) reaction mechanism. The simplified mechanism assumes that hydrolysis and P_i release are >100 s^{-1}, which has been confirmed by direct measurement (De La Cruz et al., 1999).

$$AM + ATP \underset{}{\overset{K'_1 k_2}{\rightleftharpoons}} AM.Products \underset{k_{-5}}{\overset{k_{+5}}{\rightleftharpoons}} AM + Products$$

Scheme 2

Steady-state ATPases

The steady-state ATPase activity was measured with [γ-^{32}P]ATP (Pollard and Korn, 1973) or by fluorescence, using the NADH-coupled assay (Furch et al., 1998) at 25°C in KMg50 buffer with an Applied Photophysics (Surrey, UK) SX.18MV stopped-flow apparatus. Monitoring NADH oxidation by absorbance at 340 nm gave essentially the same results as fluorescence (not shown). Myosin V-1IQ (~10 μM) was pretreated with apyrase (0.02 U ml^{-1} for 30 min.) to remove contaminating ADP. The reaction was initiated by mixing 0.4 or 4 mM MgATP with an equal volume of actomyosin (40 or 90 nM myosin and a range of actin concentration) in 2× reaction mix (400 μM NADH, 1 mM phosphoenolpyruvate, 40 U ml^{-1} lactate dehydrogenase, 200 U ml^{-1} pyruvate kinase, KMg50 buffer). The background contribution from actin and apyrase in the absence of myosin was minimal (<1%) and was subtracted from the time courses.

Duty ratio measurements (steady state)

The fraction of strongly bound myosin V-1IQ heads was determined from the amplitude of pyrene-actin fluorescence quenching immediately after

---

TABLE 1 Rate constants of the monomeric myosin V ATPase cycle

Parameter	Value	Reference
Turnover rate (V_{max})	15 s^{-1}	De La Cruz et al. (1999)*
	14.9 s^{-1}	Fig. 4, this report
	3.3 s^{-1}	Trybus et al. (1999)[†]
	3.3 s^{-1}	Wang et al. (2000)[‡]
ATP binding ($K'_1 k'_2$)[§]	0.7 μM^{-1} s^{-1}	De La Cruz et al. (1999)
	0.7 μM^{-1} s^{-1}	Trybus et al. (1999)
	0.23 μM^{-1} s^{-1}[¶]	Wang et al. (2000)
ADP binding (k'_{-5})	13 μM^{-1} s^{-1}	De La Cruz et al. (1999)
	~9 μM^{-1} s^{-1}[‖]	Trybus et al. (1999)
	15 μM^{-1} s^{-1}[‖]	Wang et al. (2000)
ADP release (k'_{+5})	16 s^{-1}	De La Cruz et al. (1999)
	~14 s^{-1}	Trybus et al. (1999)
	11.5 s^{-1}	Wang et al. (2000)
ADP affinity (K'_5)	0.9 μM	De La Cruz et al. (1999)
	2 μM	Trybus et al. (1999)
	0.77 μM	Wang et al. (2000)

*50 mM KCl, 1 mM MgCl$_2$, 1 mM EGTA, 1 mM DTT, 10 mM imidazole (pH 7.0), 25°C.

[†]100 mM KCl, 5 mM MgCl$_2$, 1 mM EGTA, 1 mM DTT, 10 mM HEPES (pH 7), 20°C.

[‡]100 mM KCl, 2 mM MgCl$_2$, 0.1 mM EGTA, 1 mM DTT, 10 mM MOPS (pH 7.0), 20°C.

[§]Rate constants are defined as in Scheme 1.

[¶]Calculated from figure 9 of Wang et al., which shows 200 μM ATP dissociating actomyosin V at a rate of 45.8 s^{-1}.

[‖]These values were calculated from the reported ADP release rates and affinities because they were not reported (Wang et al., 2000) or because they were at variance with the measured dissociation rate constant and equilibrium binding affinity (Trybus et al., 1999).

the addition of 2 mM MgATP to actomyosin V-1IQ in KMg50 buffer treated with apyrase to remove contaminating ADP. The extent of fluorescence quenching of pyrene actin is linearly proportional to the amount of myosin V-1IQ bound to the actin (De La Cruz et al., 1999). The value for 100% strongly bound myosin V-1IQ was obtained from the maximum quenching in the absence of ATP. The fluorescence of pyrene-actin in the absence of myosin V-1IQ was taken to be 0% strongly bound heads.

RESULTS AND DISCUSSION

Transient and steady-state ATP hydrolysis by myosin V

We obtained the time course of the transient and steady-state phases of ATP hydrolysis by quench flow kinetic methods (Fig. 1). The initial rapid burst of P_i production observed within the first 50 ms of the time course (Fig. 1, *inset*) is due to the rapid hydrolysis of ATP that occurs before the rate-limiting step in the cycle (Scheme 1). The burst is followed by a slower linear phase and, on a longer time scale, a nonlinear phase. The linear phase that occurs within the first 150 ms is the true steady-state myosin V-1IQ ATPase rate, and the slower nonlinear phase is due to the progressive inhibition of the ATPase activity by ADP and subsequent depletion of ATP. We modeled the kinetic profile using rate constants determined independently (De La Cruz et al., 1999) for ATP binding ($K_1 k_2'$), ADP dissociation (k_{+5}'), and ADP binding (k_{-5}'; Scheme 1 and Fig. 1). The simulated transient shows clearly that the true steady-state ATPase rate can only be determined by the acquisition of
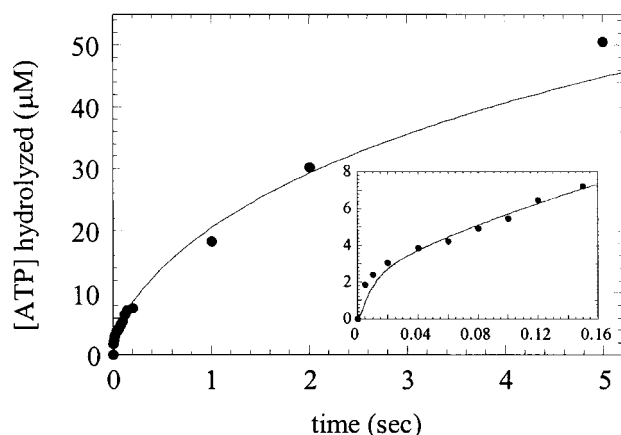
rapid time points before the ADP reaches a concentration that effectively competes with ATP. As discussed by De La Cruz et al. (1999), a high ADP affinity and rapid rate of ADP binding are responsible for the inhibition.

Simulation of transient and steady-state time courses

We performed kinetic simulations to determine the effect of product inhibition as a function of assay time and ATP concentration at a very low (20 nM) myosin V-1IQ concentration and saturating actin (Fig. 2). These simulations serve as a helpful guide for determining the most appropriate conditions for the assay of myosin V ATPase activity. A simplified two-state model that assumes ATP hydrolysis and P_i release are >100 s^{-1} (De La Cruz et al., 1999) and ADP release is slow (Table 1) and rate-limiting (De La Cruz et al., 1999) requires only the rate constants for ATP bind-
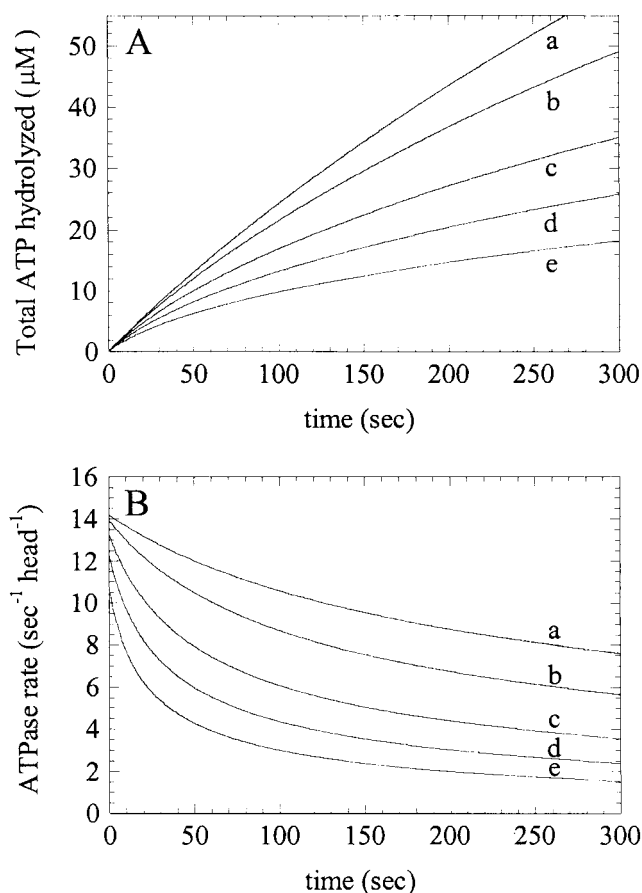

FIGURE 2 Simulations of myosin V steady-state ATPase activity. (*A*) Simulated time courses of ATP hydrolysis by 20 nM myosin V at (*a*) 1 mM, (*b*) 500 μM, (*c*) 200 μM, (*d*) 100 μM, and (*e*) 50 μM MgATP with an (initial) [ADP] of zero. (*B*) Effective ATPase rate as a function of assay time (20 nM myosin V). The curves are labeled as in *A*. Note that at <200 μM ATP, the initial V_{max} is partially limited by ATP binding.

FIGURE 1 Time course of ATP hydrolysis by myosin V-1IQ measured by quench flow. Conditions: 50 mM KCl, 1 mM MgCl$_2$, 1mM EGTA, 1 mM DTT, 10 mM imidazole (pH 7.0), 3.2 μM myosin V-1IQ, 7.5 μM actin filaments, and 100 μM MgATP, 25°C. The solid line is a simulation using our experimentally determined rates for ATP binding, P_i release, and ADP binding. (*Inset*) The initial time course of hydrolysis, showing the P_i burst and linear phase of the steady-state ATPase rate. The data points from the inset were published by De La Cruz et al. (1999). Note that the turnover rate of $\sim$11 s^{-1} head^{-1} determined from the linear region is in close agreement with the predicted value of 12.2 s^{-1} at 100 μM MgATP (Fig. 2 B, curve d).

ing, ADP release, and ADP binding (see Experimental Procedures). The two-state model allows the steady-state parameters to be determined, using the rate constants from the three published myosin V kinetic papers (De La Cruz et al., 1999; Trybus et al., 1999; Wang et al., 2000). Simulations (Fig. 2) were performed using the rate constants of De La Cruz et al. (1999) (Table 1), which are comparable to those determined by Trybus et al. (1999) but differ from Wang et al. (2000) in the rate of ATP binding. Similar results (not shown) were obtained with a more complex model (Scheme 1), using a complete set of rate constants (De La Cruz et al., 1999).

There is clearly a dramatic reduction in the ATPase rate within minutes of initiation of the assay (Fig. 2). Inhibition occurs with ATP concentrations as high as 1 mM. Published reports (Wang et al., 2000) used ATP concentrations as low as 200 μM (Fig. 2, curve c) and have most likely underestimated the true steady-state ATPase rate (see also Fig. 3, discussed below). The inhibition is even more dramatic with a slower ATP binding rate (Table 1; Wang et al., 2000), because the inhibition results from the inability of ATP to compete with a high rate of ADP binding.

Note that the true steady-state ATPase rates can be determined if measurements are made before the ADP concentration is high enough for it to effectively compete with ATP (Fig. 2 A). Under standard assay conditions (Trybus et al., 1999; Wang et al., 2000), inhibition occurs within the first few seconds of turnover (Fig. 2 B). It is important to stress that after 60 s the time courses appear to be linear (Fig. 2 A) and can be incorrectly analyzed as being the true

steady-state rate (Fig. 2 B). Others have reported the requirement for the removal of contaminating ADP from ATP stock solutions (Wang et al., 2000), as we do when necessary (see Experimental Procedures). However, it is equally important to recognize the need for measuring the steady-state ATPase rate on a rapid time scale before inhibition by ADP.

Limitations of assay methods

Typically, the steady-state ATPase rate is measured over a time course of several minutes, using radioactive (Pollard and Korn, 1973) or colorimetric (White, 1982) assays. The most commonly used method for the assay of radioactive inorganic P_i (used by Wang et al., 2000) has a minimum detection limit of 2–4 nmol (Pollard and Korn, 1973), while a colorimetric assay (used by Trybus et al., 1999) is less sensitive and has a minimum detection limit of 25 nmol (White, 1982). Assuming standard assay conditions and volumes (Pollard and Korn, 1973; White, 1982), the minimum assayable concentration is ~2 μM P_i for the radioactive assay and 30 μM for the colorimetric assay. As seen from the simulated time courses (Fig. 2), after 4 μM ATP is hydrolyzed, the ATPase is already significantly inhibited over a broad range of ATP concentrations. Using the myosin and ATP concentrations of Wang et al. (2000) and assuming that the steady-state actin-activated ATPase rate was measured over a period of 20–300 s, simulations (Fig. 2) of the time courses predict steady-state ATPase rates of 2.3 s^{-1} (using the rate constants obtained by Wang et al. (2000)) and 3.5 s^{-1} (using the rate constants of Trybus et al. (1999)), even though ADP release is rate limiting at 11.5 s^{-1} or 14 s^{-1}, respectively.

To demonstrate that the low ATPase rates can be accounted for by the accumulation of ADP, we measured the steady-state ATPase rate of myosin V-1IQ (Fig. 3) under the conditions of Wang et al. (2000), using the radioactive (Pollard and Korn, 1973) and the NADH-coupled (Furch et al., 1998) assays (Fig. 3). Unlike the radioactive assay, the NADH-coupled assay utilizes an ATP-regenerating system that prevents the accumulation of ADP. Both time courses appear linear during the experiments, but they yield dramatically different ATPase rates (Fig. 3). The radioactive assay generates a turnover rate of 4.0 s^{-1} when the data are fit over a range of 60–300 s. Note that the intercept of the fit clearly deviates from the origin. This apparent ATPase rate is comparable to the rates reported by Trybus et al. (1999) and Wang et al. (2000). In contrast, the NADH-coupled assay yields a steady-state turnover rate of 12 s^{-1}, which is the true steady-state rate at 0.2 mM MgATP (Fig. 2 B). The simulations (Fig. 2) and measured time courses (Figs. 1 and 3) show clearly that one cannot determine the rate-limiting step accurately without assaying the steady-state ATPase on a rapid time scale before inhibition by ADP or by using an
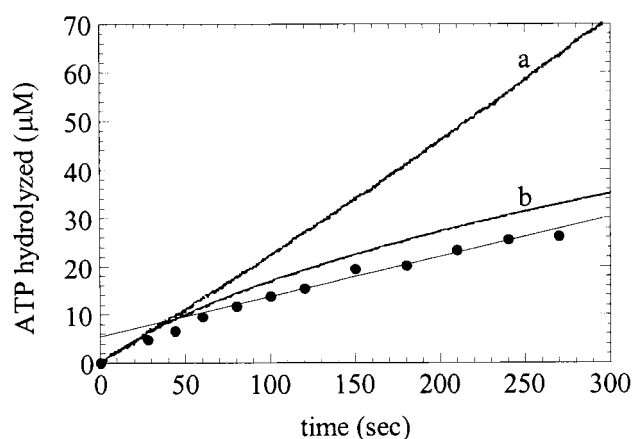

FIGURE 3 Direct comparison of ATPase assay methods. Conditions: 50 mM KCl, 1 mM MgCl$_2$, 1 mM EGTA, 1 mM DTT, 10 mM imidazole (pH 7.0), 20 nM myosin V-1IQ, 15 μM actin, 0.2 mM MgATP, 25°C. Curve a is the steady-state ATPase rate measured using the NADH-coupled assay or (●) from $^{32}P_i$ liberation. Curve b is a simulation of the predicted time course, using Scheme 2 (curve c in Fig. 2). The straight line through the data points represents the best linear fit from 60 to 300 s and yields a turnover rate of 4.0 (± 0.1) ATP s^{-1} head^{-1}. The NADH-coupled assay (curve a) yields an ATPase rate of 12 ATP s^{-1} head^{-1}.

ADP buffer to maintain a low steady-state ADP concentration (Fig. 3, *curve a*).

Time courses of steady-state ATPase activity measured in the presence of 2 mM MgATP with the NADH-coupled assay are also linear (Fig. 4). Product inhibition is not observed because ADP does not accumulate to levels that compete with the ATP in the medium (2 mM). By HPLC (not shown) we measured ~ 7 μM ADP at equilibrium under our assay conditions of 2 mM ATP, so the maximum ATPase rate measured approximates the true steady-state turnover number (Fig. 2 *B*). The V_{max} of actomyosin V-1IQ is 14.9 ($\pm$ 0.8) s^{-1} head^{-1} (Table 1), and the K_{ATPase} is 1.5 ($\pm$ 0.4) μM, in agreement with our earlier measurements (De La Cruz et al., 1999).

Implications for the myosin V duty ratio

While there may be minor kinetic differences between the chicken (De La Cruz et al., 1999) and mouse (Trybus et al., 1999; Wang et al., 2000) myosin V isoforms, rate-limiting P_i release, rather than ADP release, is not consistent with a high duty ratio motor. While P_i release could be slower than ADP release and account for the observed steady-state rates (simulations not shown) of Wang et al. (2000) and Trybus et al. (1999), such a myosin would spend most of its time in weakly bound or detached states (Scheme 1), like skeletal muscle myosin II. For instance, a P_i release rate of 3.3 s^{-1} and an ADP release rate of 11.5 s^{-1} (Wang et al., 2000) or ~ 14 s^{-1} (Trybus et al., 1999) predicts a duty ratio of ~ 0.2 that is independent of actin concentration (at [Actin] > 5 μM). However, this low duty ratio appears to be inconsis-

tent with motility assays by Wang et al. (2000) showing that myosin V translocates actin filaments at very low motor densities. Furthermore, because myosin V is believed to serve similar functions in all higher organisms (Titus, 1997), it is unlikely that a high duty ratio is needed to perform these functions in chicken, and a low duty ratio is sufficient in mice.

Trybus et al. (1999) conclude that myosin V has a low duty ratio, based on the observation that it does not quench pyrene actin (indicating strong binding) in the presence of ATP (figure 9 from Trybus et al., 1999). This is clearly in conflict with our conclusion (De La Cruz et al., 1999) that myosin V has a high duty ratio. However, the resolution of the apparent discrepancy stems from the actin concentration (0.5 μM) used in the quenching experiment of Trybus et al. (1999). Because the rate of myosin V entering the strong states is limited not by P_i release but by the rate of dissociated myosin V-ADP-P_i binding to actin, the duty ratio depends on the actin concentration (De La Cruz et al., 1999). In the published measurement of De La Cruz et al. (1999), a duty ratio of 0.7 was measured directly by steady-state fluorescence quenching of 7.5 μM pyrene actin. This is the predicted duty ratio if entry into the strongly bound states is limited by myosin-ADP-P_i binding to actin with a rate constant (k_{-9}) of 4.7 μM^{-1} s^{-1} (De La Cruz et al., 1999) and exit from the strongly bound states is limited by ADP release (k_{+5}') at 16 s^{-1} (De La Cruz et al., 1999) according to the relation

$$\text{Duty ratio} = (k_{-9}[\text{Actin}])/(k_{-9}[\text{Actin}] + k_{+5}') \quad (1)$$

This result was confirmed and extended by steady-state measurements of pyrene actin fluorescence quenching (proportional to the fraction of myosin strongly bound to actin) by myosin V-1IQ over a range of actin concentration in the presence of MgATP (Fig. 5). The solid line through the data represents the duty ratio calculated with Eq. 1 and our experimentally determined rate constants (De La Cruz et al., 1999).

In the experiment of Trybus et al. (1999), the actin concentration was 0.5 μM, which predicts a rate of myosin V-ADP-P_i binding to actin of ~ 2 s^{-1}. When the ADP dissociation rate of ~ 14 s^{-1} obtained by Trybus et al. (1999) is used, a duty ratio of 0.1 is expected (Fig. 5), explaining the lack of a significant steady-state pyrene-actin quenching. On the other hand, Trybus et al. (1999) conclude that $\sim 85\%$ of myosin V is weakly bound to actin in the presence of 1 mM ATP, based on a steady-state light-scattering assay at 1 μM actin at 20°C. However, given that the K_M measured is 20 μM under similar conditions (Trybus et al., 1999), it is unlikely that the light-scattering signal is due entirely to weakly bound myosin V. The light-scattering signal may be due to a combination of strongly bound myosin V resulting from contaminating ADP as well as weakly bound and strongly bound states in the cycle.
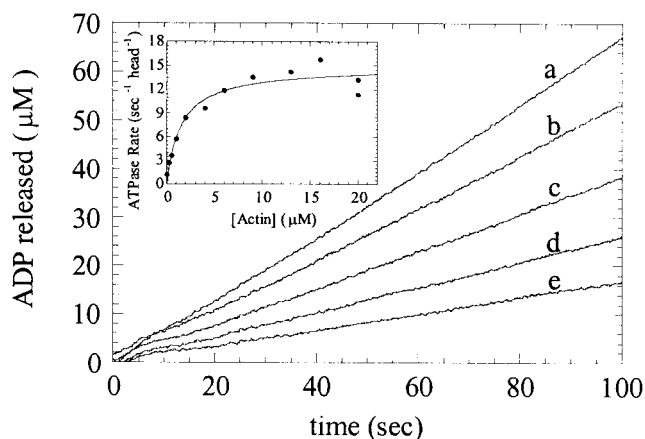

FIGURE 4 Measurement of myosin V-1IQ actin-activated ATPase activity with the NADH-coupled assay. Conditions: 50 mM KCl, 1 mM MgCl$_2$, 1 mM EGTA, 1 mM DTT, 10 mM imidazole (pH 7.0), 45 nM myosin V-1IQ, 2 mM MgATP, 25°C, and (*curve a*) 13 μM, (*b*) 6 μM, (*c*) 2 μM, (*d*) 1 μM, and (*e*) 0.5 μM actin filaments. (*Inset*) The actin dependence of the turnover number with a V_{max} of 14.9 ($\pm$ 0.8) s^{-1} head^{-1} and a K_{ATPase} of 1.5 ($\pm$ 0.4) μM obtained from the best fit of the data to a rectangular hyperbola.
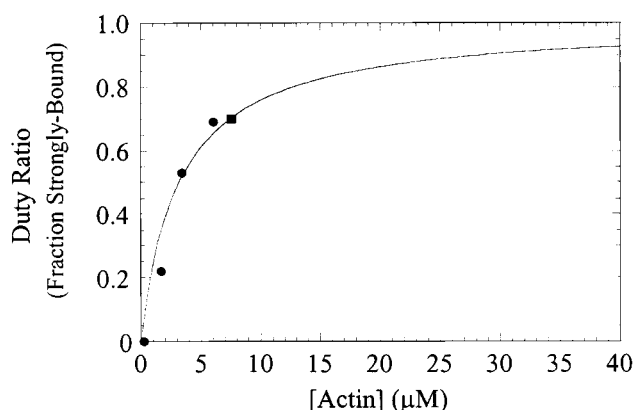
FIGURE 5 The duty ratio of myosin V-1IQ depends on the actin fila-
ment concentration. The fraction of myosin V-1IQ strongly bound to actin
was determined from the extent of fluorescence quenching in the presence
of 2 mM (●) or 100 μM (■) MgATP. The solid line through the data
represents the duty ratio calculated with Eq. 1 and our experimentally
determined rate constants for ADP release and ADP-P$_i$-myosin V-1IQ
binding to actin filaments (De La Cruz et al., 1999). Conditions: 50 mM
KCl, 1 mM MgCl$_2$, 1 mM EGTA, 1 mM DTT, 10 mM imidazole (pH 7.0),
25°C.

It is important to note that the myosin V-1IQ isoforms of
Trybus et al. (1999) and Wang et al. (1999) have a bound
calmodulin light chain rather than the essential light chain
(LC-1sa) used in our investigations. Therefore, it is possible
that there are differences in the myosin V-1IQ-calmodulin
kinetics that may result in a slightly different actin depen-
dence of the duty ratio. However, given the similarity in the
reported rate constants (Table 1), it is unlikely that calmod-
ulin changes the rate-liming step from ADP release to
phosphate release.

Relationship to other myosins

Other unconventional myosins have high ADP affinities and
association rates, including two isoforms of myosin I, *myr-1*
(Coluccio and Geeves, 1999) and brush-border myosin I
(Jontes et al., 1997). In such cases, our simulations for
myosin V demonstrate the need for the measurement of
steady-state ATPase rates under conditions where product
inhibition is not a potential problem. However, because the
measured steady-state rates for actomyosin I are slow and
~10-fold lower than the rate of ADP dissociation, it is
unlikely that concentrations of ADP needed for a 10-fold
level of inhibition accumulate over the time course of a
standard steady-state assay. Nevertheless, it may be neces-
sary to determine the steady-state rates of these myosins in
the absence of potentially inhibiting concentrations of ADP.
This can be done either by making rapid quench flow
measurements or by using an ADP buffering system (Fig.
3). In addition, the P$_i$ release rate should be measured

directly and not be assumed to be limiting the steady-state
turnover rate.

In summary, the most plausible interpretation is that the
actin-activated cycle of myosin V is limited by the rate of
ADP release. Consequently, myosin V has a high duty ratio
that depends on the actin filament concentration, consistent
with the native, two-headed molecule being processive on
actin filaments. While we cannot rule out isoform properties
leading to kinetic differences, it is likely that any such
differences will be minor, given that the myosin V class of
motors is thought to fulfill similar cellular roles in all higher
organisms. It is much more likely that the apparent discrep-
ancies in the three reports on the kinetics of myosin V stem
from the difficulty of measuring the steady-state ATPase
activity.

REFERENCES

Coluccio, L. M., and M. A. Geeves. 1999. Transient kinetic analysis of the
130-kDa myosin-I (MYR-1 gene product) from rat liver. *J. Biol. Chem.*
274:21575–21580.

De La Cruz, E. M., A. L. Wells, S. S. Rosenfeld, E. M. Ostap, and H. L.
Sweeney. 1999. The kinetic mechanism of myosin V. *Proc. Natl. Acad.
Sci. USA.* 96:13726–13731.

Furch, M., M. Geeves, and D. J. Manstein. 1998. Modulation of actin
affinity and actomyosin adenosine triphosphatase by charge changes in
the myosin motor domain. *Biochemistry.* 37:6317–6326.

Jontes, J. D., R. A. Milligan, T. D. Pollard, and E. M. Ostap. 1997. Kinetic
characterization of brush border myosin-I ATPase. *Proc. Natl. Acad. Sci.
USA.* 94:14332–14337.

MacLean-Fletcher, S., and T. D. Pollard. 1980. Identification of a factor in
conventional muscle actin preparations which inhibits actin filament
self-association. *Biochem. Biophys. Res. Commun.* 96:18–27.

Mehta, A. D., R. S. Rock, M. Rief, J. A. Spudich, M. S. Mooseker, and
R. E. Cheney. 1999. Myosin-V is a processive actin-based motor.
Nature. 400:590–593.

Mooseker, M. S., and R. E. Cheney. 1995. Unconventional myosins. *Annu.
Rev. Cell Dev. Biol.* 11:633–675.

Pollard, T. D., and E. D. Korn. 1973. Acanthamoeba myosin. I. Isolation
from *Acanthamoeba castellanii* of an enzyme similar to muscle myosin.
J. Biol. Chem. 248:4682–4690.

Titus, M. A. 1997. Motor proteins: myosin V—the multi-purpose transport
motor. *Curr. Biol.* 7:R301–R304.

Trybus, K. M., E. Krementsova, and Y. Freyzon. 1999. Kinetic character-
ization of a monomeric unconventional myosin V construct. *J. Biol.
Chem.* 274:27448–27456.

Wang, F., L. Chen, O. Arcucci, E. V. Harvey, B. Bowers, Y. Xu, J. A.
Hammer, and J. Sellers. 2000. Effect of ADP and ionic strength on the
kinetic and motile properties of recombinant mouse myosin V. *J. Biol.
Chem.* 275:4329–4335.

White, H. D. 1982. Special instrumentation and techniques for kinetic
studies of contractile systems. *Methods Enzymol.* 85:698–708.